



A Response Surface Approximation for the Bench-Scale Peak Heat Release Rate from Upholstered Furniture Exposed to a Radiant Heat Source

S. L. Thompson & G. E. Apostolakis*

School of Engineering and Applied Science, University of California, Los Angeles,
California 90024-1597, USA

(Received 3 January 1991; revised version received 14 February 1993; accepted 4 April 1993)

ABSTRACT

This work investigates the initial stages of a residential fire scenario: specifically the peak heat release rate (kW/m^2) from an item ignited by exposure to a radiant heat source. Parameters which may define a scenario include the material properties of the furniture and the ignition source. The emphasis is on the uncertainties in these parameters and their impact on the peak heat release rate (kW/m^2). A response surface analysis is performed to determine the equivalent bench-scale heat release as a function of fabric, padding, oxygen concentration, and imposed radiant heat flux. A response surface is a polynomial which approximates the computer code and it may be used to predict heat release values, as well as the uncertainties in these values due to uncertainties in the model input variables.

1 INTRODUCTION

Assessing the risk from fires consists of the calculation of the probability of consequences, i.e. death, injury or property loss, occurring from some defined fire hazard. Fire risk models have been developed for use in the nuclear industry¹ and a method for modeling the risk of deaths from fires in buildings has been presented in Ref. 2. All of these models involve the assessment of the probability distributions of the initiation and propagation of the fire and consequences due

*To whom correspondence should be addressed.

to the first. After the ignition of the first item, the processes of fire growth, detection and suppression interact to produce a variety of possible scenario outcomes. These outcomes may be predicted by characterizing the scenarios according to the parameters which may change the course of the fire, and thus change the end risk to persons or property. Parameters which may define a scenario include the material properties of the furniture and the ignition source. Material properties may include: ignition resistance, the rate of heat release, and the characteristics of the combustion products.

In Refs 3–5, various scenarios involving an upholstered furniture item exposed to a radiant flux from a variety of heaters, i.e. electric, wood and gas, are defined. Physical models of the heat transfer processes are coupled with an uncertainty analysis of the parameters in the models and a probabilistic analysis of the events involved in a typical scenario. This leads to a distribution of the frequency of ignition of the furniture due to exposure to a heater. The first step in a PRA (probabilistic risk assessment) is, then, performed by defining these scenarios and assigning probabilities to them. The second step of a PRA, the calculation probabilities to them. The second step of a PRA, the calculation of the fire growth time (T_G), is a more difficult task. This task is begun in Refs 3–5 through the development of a computer model to calculate the time to ignition, given a specific scenario involving heat type and the type and placement of the upholstered item.

The fire growth time may be determined by several computer codes, such as, HAZARD 1⁶ and FAST/FFM.^{7,9} The latter code is a sophisticated tool that provides time-dependent predictions of furniture fire growth, as well as information on the spread of smoke and fire to other rooms. Distributions of the output reflecting the uncertainties in the input parameters may only be constructed through costly Monte Carlo simulation. The purpose of this paper is to discuss the propagation of uncertainty, as it is required in risk assessment, and to present a method for obtaining analytical approximations ('response surfaces') to the output of the fire growth portion of computer codes, so that many of the calculations required for risk assessment may be performed without the use of these computer codes. In this paper, a response surface is developed to predict the bench-scale heat release rate (kW/m^2) from a fire, which can be used in full-scale correlations when test data are not available. For the purposes of this paper, simple fire spread models are employed that are deemed satisfactory for the basic scenario being analyzed. For a more realistic analysis of furniture fires, one would have to apply the methods of this paper to a more advanced code, such as FAST/FFM.

Section 2 discusses parameter uncertainties and introduces the concept of response surfaces as approximations to computer codes. Section 3 introduces the scenario of interest in this work. The equations used to calculate the heat released from the fire are given in Section 4, while Section 5 lists the equations for vertical and horizontal flame spread. Section 6 contains the response surface for the bench-scale peak heat release rate and, finally, Section 7 offers some concluding remarks.

2 RESPONSE SURFACES

One of the parameters necessary to the performance of a fire risk assessment is the growth time of a fire. This time may be called an estimate of the deterministic reference model (DRM), e.g. the computer code that may be used, and there are two kinds of state-of-knowledge uncertainties associated with it: parameter and model uncertainty. The parameter uncertainty is uncertainty in the input to the code and model uncertainty is due to the fact that physical processes may not be modeled exactly and simplifying assumptions must be made.

This paper deals with parameter uncertainties. Significant uncertainties exist in the input parameters to the DRM, including thermal properties of furniture materials, as well as other combustibles. Lack of experimental evidence and knowledge of the composition of these materials contributes to this uncertainty. Methods for propagating the parameter uncertainties through the DRM include, Monte Carlo, Latin Hypercube Sampling, and Response Surfaces. The latter is the subject of this paper and is discussed next.

A response surface is a convenient approximate solution used when the inputs to the problem are uncertain and no analytical solution exists. The application of response surface methodology establishes which of the independent variables, X_i , have the greatest effect on the solution variables, Y , and then replaces the complex computer model by a simple function which provides a reasonable representation of the true function.^{10,11} The response surface usually takes the form of a polynomial:

$$Y = \beta_0 + \sum \beta_i X_i + \sum \sum \beta_{ij} X_i X_j + \sum \beta_{ii} X_i^2 + \dots \quad (1)$$

This mathematical function is good for a range of independent variables in the problem. Methods of structuring the code runs so that the range of each independent variable is sampled include factorial and

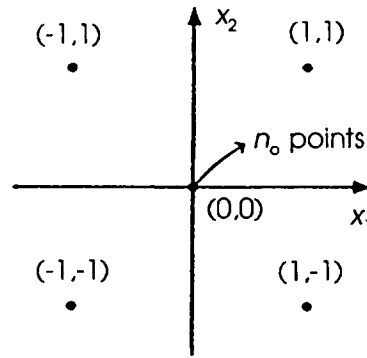


Fig. 1. Addition of center points to a 2^2 factorial design.¹¹

composite designs. A factorial design is the most basic method, in which the variables are assigned two values corresponding to the highest and lowest in their range. Central points may be added to this design to reduce the error incurred when fitting the surface to the data (Fig. 1). When performing this analysis, the variables are normalized on an interval $(-\alpha, \alpha)$ (eqn (2)), where α is often chosen so that the normalized variable range lies in the interval $(-1, 1)$:

$$XI = 2\alpha(X - X_{\text{low}})/(X_{\text{high}} - X_{\text{low}}) - \alpha \quad (2)$$

where X_{high} and X_{low} are the high and low range values for X . Uncertainties in the variables may be propagated through the response surface to obtain the uncertainty in the final solution.

3 SCENARIO CHARACTERIZATION

A necessary step in the calculation of the growth time of a fire is to obtain a heat release rate curve which is scenario-dependent. Full-scale heat release rate (kW) curves are needed to predict the progress of the fire in a room and they are often required as input to compartment fire models. Correlations exist which can predict a triangular heat release curve, if a value of the bench-scale release rate (kW/m²) is known from furniture calorimeter data. Experimental values of the bench-scale rate of heat release are not known for all fabric/padding combinations; therefore, a computer code has been developed in this work to simulate flame spread over a portion of an upholstered item and predict the equivalent bench-scale rate of heat release. The equations used to calculate the heat release from the fire are given in Section 4. The heat release of the upholstered item is a function of its fabric and padding as well as the applied heat flux from the heater. Parameter values for

even one fabric/padding combination are very uncertain. Material properties must be determined experimentally and are not accurate, or even known for all combinations. Due to these uncertainties, the calculated heat release rate (kW/m^2) will also have uncertainty associated with it.

The heat released from the fire is used as input to the equations of flame spread to calculate the spread of the fire in a given time interval. The equations used to calculate vertical and horizontal flame spread are listed in Section 5. The equations used to calculate the maximum heat release rate are very complex and, as discussed above, produce uncertain results because of uncertainties in the input parameters. For these reasons, a response surface analysis is performed on the output of the code, the maximum rate of heat release.

4 HEAT RELEASE

The full-scale peak heat release rate is important in the modeling of upholstered furniture fires, especially as pertaining to risk calculations. A heat release rate model is required for a fire risk analysis and is standard input for compartment fire codes. Typical heat release rate curves for upholstered furniture may often be approximated by a simple triangular representation of the curve shape.¹² The important features of this model are the peak release height, the base width, and the time from ignition to the start of the triangular burning region. This start-up time has not only been found to be a function of the properties of the furniture, but also to depend strongly on the ignition sequence.

For the ignition sequence in Refs 3–5, radiant ignition, the furniture is preheated to the extent that, at the time of ignition, the temperature gradients beneath the surface are very small. Due to the elevated temperatures below the ignited portion, there is very little heat loss to the padding and the fire progresses very rapidly, leading to a steep heat release curve almost from the onset of ignition. This means that, in the case of radiant ignition, the triangular portion of the curve begins at the time of ignition.

Two correlations exist for the full-scale peak heat release rate (kW), one based on bench-scale testing and the other based solely on materials identification, intended for use when destructive testing is not feasible.^{12,13} The method based on bench-scale testing is preferred, since the effects of fire retardants or other fabric treatments can be assessed through experimentation. The ability to utilize furniture calorimeter data to represent the release rates (kW/m^2) in room fires can only be applied to 'fuel limited' or 'surface' controlled burning. 'Ventilation'

controlled burning, or fires with no excess oxygen in the combustion gas stream, cannot be represented by such simple models.

At present there is no furniture calorimeter data based on the scenario described in Refs 3–5; therefore, to be able to use the preferred method of heat release estimation, it is necessary to develop a predictive model for the maximum heat release rate (kW/m^2). The model that has been developed utilizes flame spread theory and the heat release at each time step in the flame spread model is calculated by the following equation.^{13,14}

$$q''_{\text{chem}} = \eta \dot{m}'' H_c \quad (3)$$

where η is the burning efficiency; and H_c is the heat of combustion.

The mass burning rate term is calculated from the following equation:

$$\dot{m}'' = (q''_F + q''_E - q''_L) / L_g \quad (4)$$

where q''_F is the radiative heat flux from the flame to the surface; q''_E is the heat flux from the heater to the surface; q''_L is the surface heat losses (reradiation + convection); and L_g is the effective heat of gasification of the fuel.

Radiation from the flame to the surface is calculated from the heat release of the previous time step:¹⁵

$$q''_F = x_R x_p q''_{\text{chem}} / 2x_f \quad (5)$$

where x_R is the fraction of heat released as radiation; x_p is the pyrolysis length; x_f is the flame length; and q''_{chem} is the chemical heat release rate (eqn (3)).

The heat loss from the surface, q''_L , is:^{13,14}

$$q''_L = \varepsilon \sigma (T_s^4 - T_\infty^4) + h(T_s - T_f) \quad (6)$$

where h is the convective heat transfer coefficient; T_s is the surface temperature; T_f is the flame gas temperature; ε is the emissivity of the surface; σ is Stefan–Boltzmann constant ($5.67 \times 10^{-8} \text{ W/m}^2\text{K}^4$); and T_∞ is ambient temperature.

In-depth conduction into the solid is neglected in the heat loss term, because the surface has been preheated; reflected radiation is also neglected.

5 FLAME SPREAD MODELS

The orientation of a burning surface has a profound effect upon the rate of flame spread. The rate of flame spread has been found to increase

dramatically with angle of inclination. Low rates of flame spread have been found for vertically downward spread, with rates increasing for horizontal flame spread and the highest flame spread rates occurring with vertically upward flame spread. The controlling mechanism in horizontal and downward flame spread is conduction through the solid and flame spread behaves as predicted by a simple energy balance on the fuel surface. The controlling mechanisms for vertically upward flame spread, however, are radiation from the flame and, to a lesser extent, convection from hot gases. This is due to the fact that the flame lies close to the vertical surface and the hot gases are trapped between the flame and the fuel, whereas, in horizontal and downward spread, the flame and the hot gases rise upward and away from the fuel surface.

Although vertically upward flame spread may be expressed by the same basic energy balance as performed for horizontal spread, quantities in the analysis, such as the pyrolysis length and the heat flux to the fuel, are much more difficult to estimate. The pyrolysis length and the flame height appear to grow exponentially with time and the heat flux over the preheated region is usually a function of position. These complications make the development of correlations for vertical spread more difficult and the equations presented for vertical spread are based on an analysis of the exact boundary layer equations.

5.1 Horizontal and downward flame spreads

Horizontal and downward flame spreads can be grouped together as examples of opposed flow spreads, which refers to the presence of an external air flow in the direction opposite to the spread of the flame. These air flows may include buoyancy induced flows or forced flows.

For materials thicker than 2 cm, conduction through the solid has been found to be the dominant mode of heat transfer. This has been shown for downward flame spread over thick PMMA rods¹⁶ and for horizontal flame spread over thick PMMA sheets.¹⁷ Radiation from the flame has been found to be negligible in downward flame spread due to the small view factor from the flame to the fuel. In horizontal flame spread, however, radiation may be comparable to conduction through the solid, as buoyancy raises the flames high above the fuel surface, providing a large view factor to the fuel. Flame radiation becomes increasingly dominant as the size of the fire increases. Of course, for materials with extremely large or small thermal conductivities these generalities may not apply. Conduction through the solid would not be significant for a material with a very low thermal conductivity and a material with a high thermal conductivity

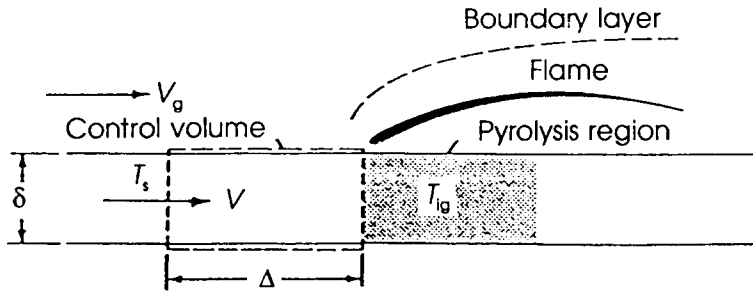


Fig. 2. Energy conservation analysis in opposed flow spread.¹³

would act as a heat sink and would actually act to prevent the spread of flame.

The fundamental equations of flame spread are based on an energy conservation analysis over a fuel control volume of thickness δ and length Δ , depicted in Fig. 2. The energy balance analysis-applied to the thermally thick case is valid with δ becoming a time dependent thermal penetration depth which can be found from heat conduction theory.¹⁸ The length scale, Δ , may be estimated from an order-of-magnitude analysis of the thermal energy equation, allowing the conduction term ($k \cdot d^2T/dx^2$) to balance the opposed flow convection term ($\rho c \cdot dT/dx$) which yields a value for $dx \approx \Delta$.¹⁸ The flame spread rate for the thermally thick case becomes:¹⁹

$$V = V_g (k\rho c)_g (T_f - T_{ig})^2 / k\rho c (T_{ig} - T_s)^2 \quad (7)$$

where k is the conductivity of the fuel; ρ is the density of the fuel; c is the specific heat of the fuel; ρ_g is the density of the gas phase; c_g is the specific heat of the gas phase; k_g is the thermal conductivity of the gas phase; T_f is the flame temperature; T_{ig} is the ignition temperature of the fuel; and T_s is the surface temperature of the unburnt fuel.

Under natural convection conditions, the ambient flow velocity, V_g , is given by:²⁰

$$V_{g \text{ nat. convection}} = [(k/\rho c)_g g (T_f - T_g) / T_g]^{1/3} \quad (8)$$

where T_g is the gas phase ambient temperature; and g is the gravitational acceleration.

5.2 Upward flame spread

Upward flame spread is an example of concurrent flow, when the buoyancy driven flow is in the same direction as that of the spread of the flame. The dominating mechanisms of concurrent flame spread are

convection and radiation from the flame to the unburnt fuel. This is because the hot combustion gases are driven ahead of the flame, close to the unburnt fuel. The unreacted gases react with the oxidizer upstream, extending the flame ahead of the pyrolysis front, where it remains very close to the unburnt material. For these reasons, this mode of flame spread occurs much more rapidly and poses greater danger than opposed flow flame spread.

An energy balance will produce the same equations given in the previous section, however, for this case, q'' will vary with the convective and radiative heat fluxes to the fuel, and Δ has been shown to depend on the length of the pyrolyzing region, x_p , to some power, n .²¹ The value of n has been found to vary from 0.5 to 1.0 for upward turbulent flame spread. Experiments with PMMA sheets²² found n to be 0.5 for the thermally thin case and 0.75 for the thermally thick case. Separate experiments on thick PMMA²³ found n to be 0.964, indicating an almost linear dependence on pyrolysis height, found to occur in turbulent flow. The latter experiments also found that upward flame spread is largely turbulent, except for an initial laminar region of about 10 cm. In this laminar region, heat transfer by convection dominates because the flame is very thin; however, radiation becomes increasingly important as the flow becomes turbulent and the flame becomes larger. Radiation from the flame has been found to account for up to 80% of the total heat transferred to the unburnt fuel at heights above 76 cm.^{23,24}

In Refs 25 and 26, the boundary layer analysis is approximated to obtain a solution for the spread of a vertical pyrolysis region. A set of algebraic correlations are presented with which values of the pyrolysis length, flame height, spread velocity, and heat flux from the flame may be calculated at various times. These equations form the basis for the development of a vertical flame spread code. The results of the analysis in Refs 25 and 26 for a free convective boundary layer are presented as follows:

The flame height, x_f , is calculated as a function of the pyrolysis length, x_p ; their ratio is a constant, β :

$$\beta = x_f/x_p = 0.64(r/B)^{-2/3} \quad (9)$$

where:

$$B = [rY_{ft}H_c - c_p(T_s - T_g)]/L_g \quad (10)$$

$$r = Y_{ox,z}/r_o Y_{ft} \quad (11)$$

and Y_{ft} is the fraction of vaporized mass that is combustible fuel; H_c is the heat of combustion; c_p is the specific heat of the solid; L_g is the heat of vaporization; T_s is the surface temperature; T_g is the ambient

temperature; r_o is the oxygen to fuel stoichiometric ratio; and $Y_{O_2,\infty}$ is the mass fraction of oxygen in the atmosphere.

At time zero, an initial ignition pyrolysis length is assumed. The pyrolysis length at successive times may be calculated by:

$$(x_p^{1/2} - x_{p,0}^{1/2}) = [4\alpha_0^2 \{1 - 1.25(r/B)^{1/3}\} / \{\pi(\rho c_p k)_s (T_s - T_g)^2\}] (t - t_0) \quad (12)$$

The flame spread velocity is then:

$$V = [8\alpha_0^2 \{1 - 1.25(r/B)^{1/3}\} / \{\pi(\rho c_p k)_s (T_s - T_g)^2\}] x_p^{1/2} \quad (13)$$

with:

$$\alpha_0 = 0.27B^{7/4} r^{0.19} L_g \rho v (h_c / v^2 c_p T_g)^{1/4} / \{(B+1)^{1/4} Pr^{1/2} \ln(B+1)\} \quad (14)$$

where all variables are as defined above, and ρ_s is the density of the fuel; ρ is the density of air; k is the thermal conductivity of the fuel; and v is the kinematic viscosity of air.

6 A RESPONSE SURFACE FOR THE MAXIMUM HEAT RELEASE RATE

A response surface has been developed to predict the maximum heat release rate from a burning cushion-like item. The equations used to calculate vertical and horizontal flame spread, and heat release, have been listed in Sections 4 and 5. The equations for vertical flame spread derived from the boundary layer equations are used to predict the initial flame spread after the ignition of a portion of furniture receiving a radiant flux from a heater. This ignition occurs due to the radiative flux from a heater, as described in Refs 3–5. This section is assumed to be 0.1 m in height (the front of a cushion) and is assumed to be the only section receiving noticeable flux from the heater. When the pyrolysis region reaches the top of the cushion, the fire is assumed to spread horizontally over the top.

The values of the inputs to the code were chosen in a factorial design with central points. The range of values represent the following fabric/padding combinations: P-C/NFR PU; P-C/FR PU; and PP/NFR PU; PP/FR PU. (Here, P-C means 65% polyester/35% cotton blend, NFR PU means non-fire-retardant polyurethane foam, FR means fire-retardant, and PP means polypropylene.) The code was run for irradiances of 20 to 40 kW/m².

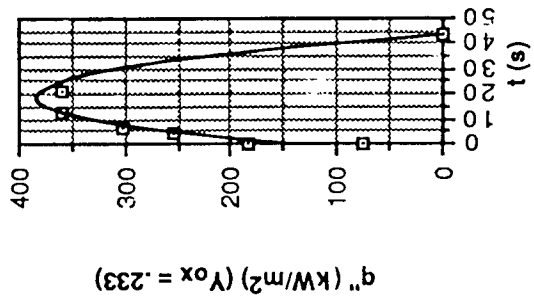
Variations in the heat release values predicted by the code can be seen in Fig. 3 [(a) P-C/NFR PU, 20 kW/m²; (b) P-C/NFR PU, 25 kW/m²; (c) PP/NFR PU, 35 kW/m²; (d) PP/NFR PU 40 kW/m²]. The values of heat release rise higher and faster with increase in the irradiance for each fabric/padding combination. However, at a given radiant heat flux, the heat release values rise much faster for the P-C combinations than for the PP combinations; this trend may be explained by an analysis of the boundary layer profiles. The PP combinations were found to have lower mass burning rates than the P-C combinations, and, thus, burned slower. The absolute values of the heat release rates were much higher for the PP combinations due to higher heats of combustion. Therefore, materials with high stoichiometric ratios and high heats of combustion burn slower but release more heat than materials with lower stoichiometric ratios and lower heats of combustion. These trends are important when a response surface is sought to approximate the computer code, generalizing the problem for a range of variable values. Figure 4 depicts the effect of oxygen concentration on the rate of heat release. A similar trend can be identified with the aid of the boundary layer profiles. Decreasing the oxygen concentration was found previously to decrease the mass burning rate, which leads to slower increases in heat release.

Comparisons of experimental data, Fig. 5, to the code output, Fig. 6, show similar trends in the initial fire growth rates. Exact curves could not be duplicated as they are extremely sensitive to the values of the input parameters. Parameter values for even one fabric/padding combination are very uncertain. Parameters such as the combination material properties must be determined experimentally and, therefore, are not accurate, or even known for all combinations.

The parameters chosen to be the independent variables of the response surface are the material properties represented by: $X1 = \rho kc$, $X2 = Y_{O_2, \infty} / r_{O_2}$, and $X3 = L_g / H_c$; and the external heat flux: $X4 = q_{ext}$. In order to create a reasonable function for the response surface, the functional dependence of the heat release rate on the independent variables must be determined. In Fig. 7, the heat release rate is plotted against the normalized parameters, $X1-X4$. It can be seen that the heat release rate varies almost linearly with $X2$ and $X3$, but seems to vary quadratically with the parameters $X1$ and $X4$. If the curves in Fig. 7 could be fit more accurately with simple polynomials, then one might expect only the linear and quadratic terms of the parameters to be important. However, it is suspected that some of the cross-product terms cannot be neglected (eqn (1)).

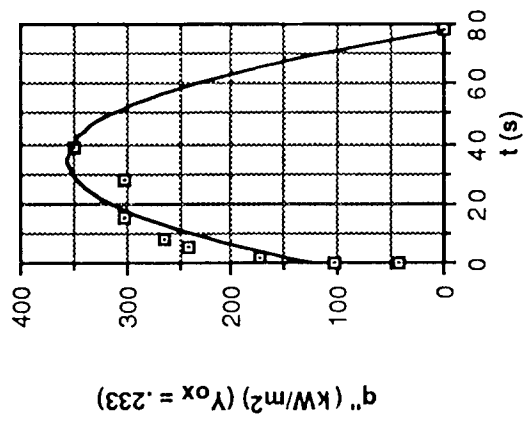
A Response Surface Analysis was performed on the normalized data

$$y = 145.7055 + 24.9562x - 0.6523x^2 \quad R = 0.97$$



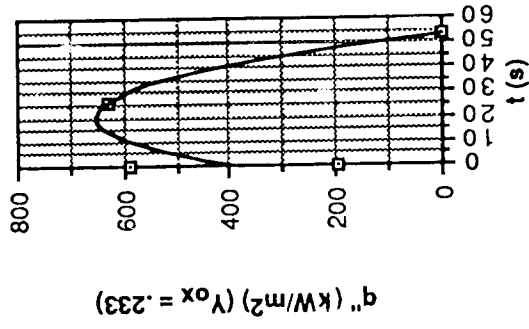
(b)

$$y = 123.498 + 13.4006x - 0.193x^2 \quad R = 0.94$$



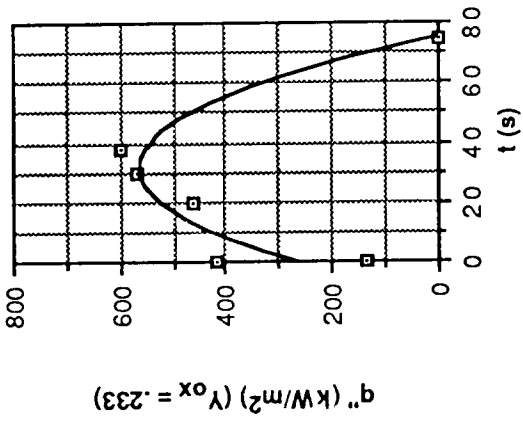
(a)

$$y = 391.9675 + 25.4045x - 0.6189x^2 \quad R = 0.85$$



(d)

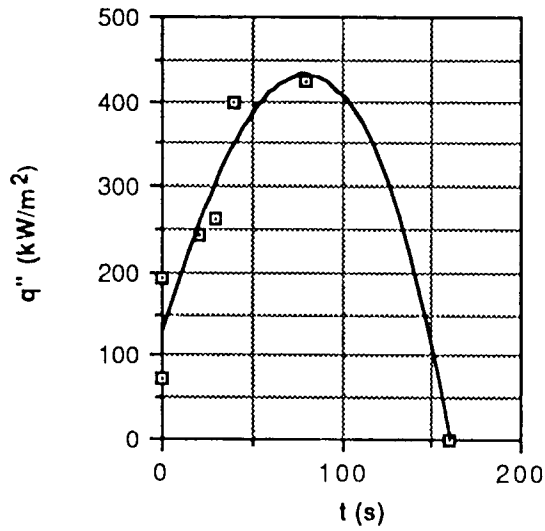
$$y = 264.8362 + 18.8981x - 0.2977x^2 \quad R = 0.92$$



(c)

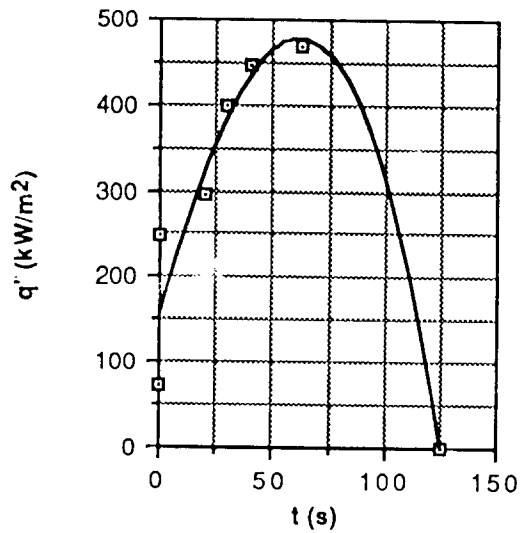
Fig. 3. Effect of material and irradiance on heat release rate curves: (a) P-C/NFR PU, 20 kW/m²; (b) P-C/NFR PU, 25 kW/m²; (c) PP/NFR Pu, 35 kW/m²; (d) PP/NFR Pu, 40 kW/m². (Note that y = q'' and x = t.)

$$y = 129.2769 + 6.7891x - 0.0276x^2 - 1.234e-4x^3 \quad R = 0.96$$



(a)

$$y = 157.975 + 9.3342x - 0.0498x^2 - 2.815e-4x^3 \quad R = 0.96$$



(b)

Fig. 4. Effect of oxygen concentration on heat release rate curves, PP/NFR PU, 30 kW/m²: (a) $Y_{ox} = 0.18$; (b) $Y_{ox} = 0.233$. (Note that $y = q''$ and $x = t$.)

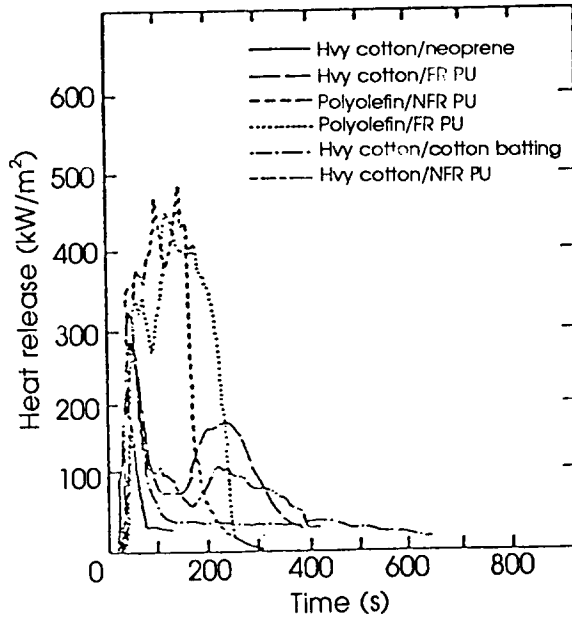


Fig. 5. Cone calorimeter measurements of the heat release rate for various fabric/padding combinations at an irradiance of 25 kW/m^2 .¹²

in Table 1 and the values for the resulting coefficients are given in Table 2. The highest order term in the equation is quadratic and all but three of the cross-product terms are included. Functional errors and statistical variances are presented in Tables 3–6. Table 3 gives the distribution of the response surface in terms of the mean and the standard deviation (root MSE). The R -square value is the coefficient of determination (correlation coefficient) and indicates the fraction of variation in the response due to the function. A value close to unity indicates high correlation. The response surface calculated has a correlation coefficient of 0.9791, which indicates that the data are highly correlated and, that the model employed is reasonable.

Table 4 indicates the relative importance of the terms in the model. The linear terms are by far the most significant, followed by the quadratic terms, with the cross-product terms contributing relatively little to the model. The Type I sum of squares measures the reduction in the error as each set of terms is added to the model. The data are highly correlated to the linear model ($R = 0.9212$) and the addition of the quadratic and cross-product terms only increases the correlation coefficient by 0.0579. The F -ratio is also an important indication of a term's significance. The probability $>F$ value is the probability that the F -ratio would have at least as great a value as the given one if the

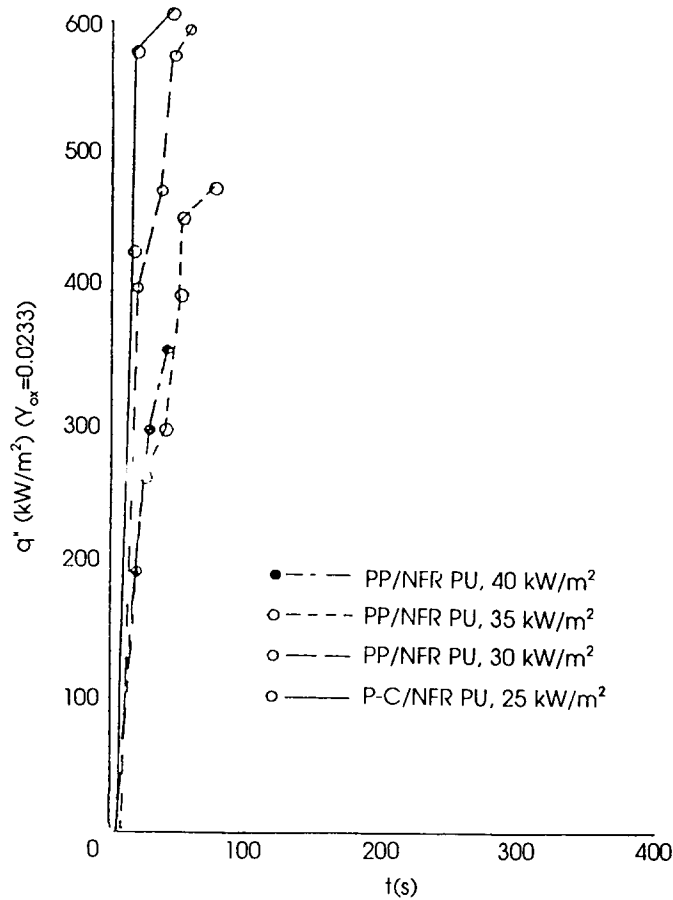


Fig. 6. Heat release rate curves for various fabric/padding combinations.

indicated terms were zero. The probability that the linear terms should be zero is very low, 0.0015, while the probability that the cross-product terms should be zero is significant, 0.8272; in fact, three of the terms are zero.

Table 5 lists the results of the same tests as Table 4, but they are performed on the individual parameters. As is already known, none of the parameters is insignificant, since the linear correlation is very high. However, the significance of the terms with respect to each other can be measured. The external heat flux appears to be the most significant parameter, followed closely by the ratio of the heat of gasification to the heat of combustion, X_3 . The least significant parameter appears to be the ratio of the ambient oxygen concentration to the stoichiometric oxygen to fuel ratio, X_2 . This makes sense since X_2 was found earlier

to affect the rate of rise more than the absolute value of the heat release rate. On the other hand, both the external heat flux and the heat of combustion were found to affect the maximum value of the rate of heat release.

Finally, the relative significance of all the terms in the model can be seen in Table 6. The least significant term appears to be the $X2 * X1$ term; it would have little effect on the dependent variable if it was removed from the model.

7 CONCLUDING REMARKS

A response surface for the determination of the maximum heat release rate has been developed to approximate a computer code. The reason for developing this approximation is not only to save man-hours and computer time in the calculation of the maximum heat release rate of a cushion-like upholstered item, but also to have a quick and reasonably accurate method of determining the uncertainty in the maximum heat release rate from the uncertainties in the parameters. All of the independent parameters that change from scenario to scenario and are input to the computer code are used as parameters for the response surface. The parameters are grouped to eliminate interdependence between them and prevent false responses from the heat release rate. The functional dependence of the maximum heat release rate on the groups of parameters chosen is as expected. The maximum heat release rate increases with increases in the external heat flux and the heat of combustion. These two parameters have the greatest effect on the maximum heat release rate, as shown in the analysis, because they affect the actual value of the heat release rate. The other two parameters define the rate of heating of the material and the rate of oxygen depletion and, thus, the rate of burning. The latter parameters have less effect on the maximum heat release rate, as they affected the rate of rise of the heat release curve, but they are still significant in the response surface and cannot be eliminated, as might be expected.

The response surface developed in this work is a reasonable approximation to the computer code for the range of parameter values studied. Heat release rates for other materials and substrates may be found from this response surface, if the parameter values lie within the range of study. Parameter values outside of the ranges of study may still be valid in the response surface, as the upper and lower ranges used have some uncertainty attached to them. The true range of parameter values which may be used in the response surface may be found from

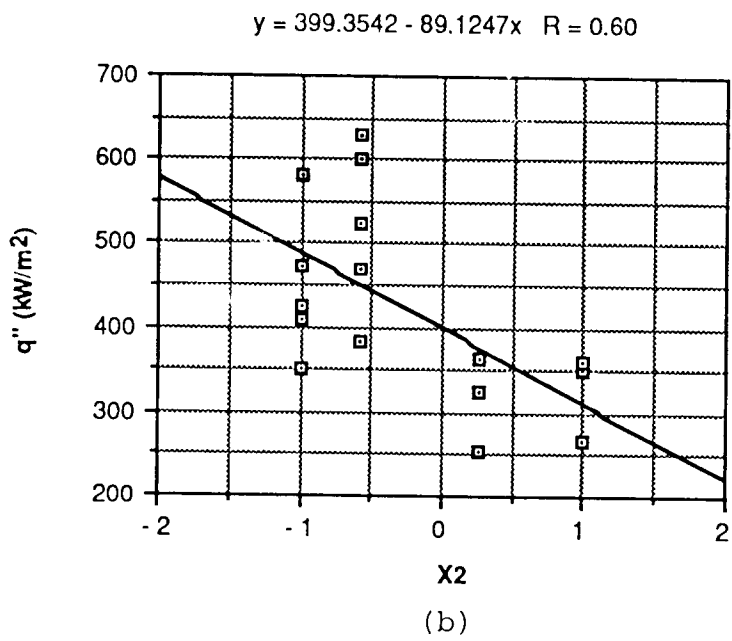
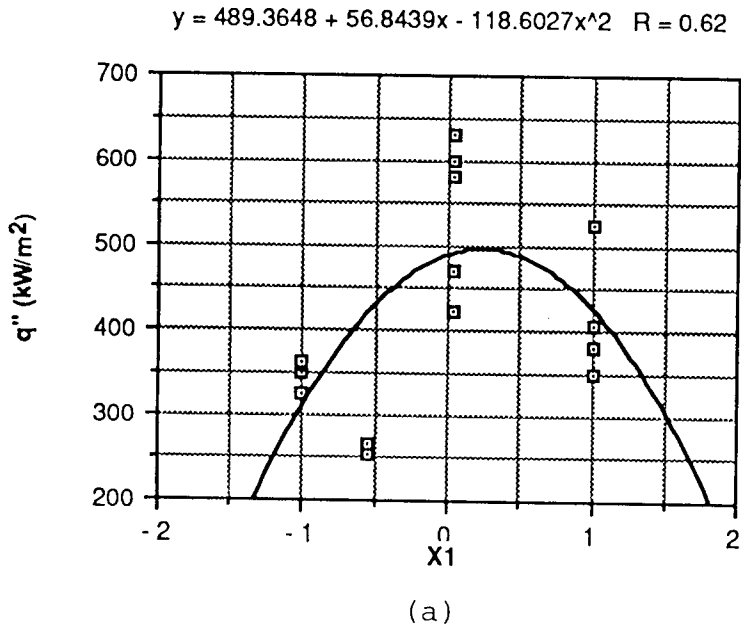
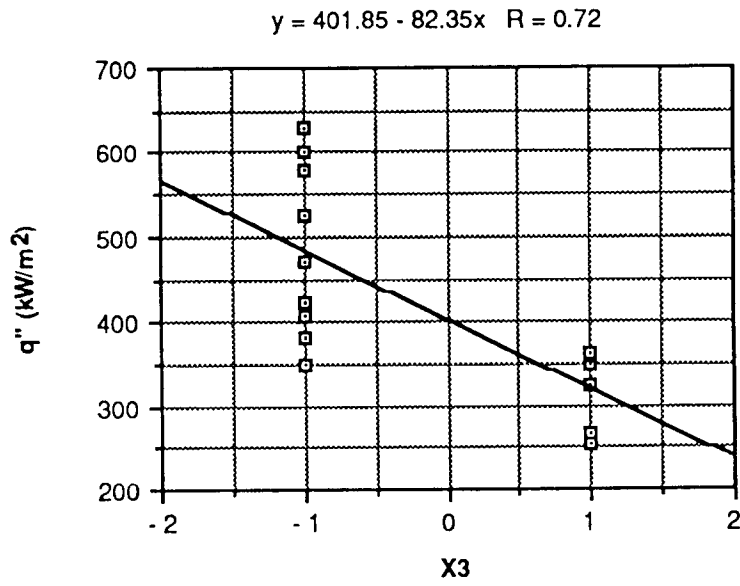
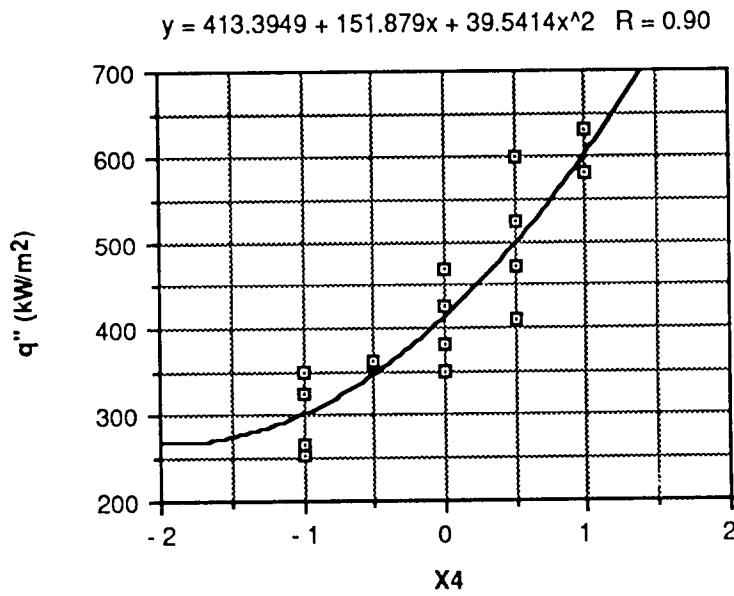


Fig. 7. Graphs of heat release rate versus model parameters (note that $y = q''$ and $x = t$). \square $q''(\text{kW}/\text{m}^2)$.



(c)



(d)

Fig. 7. (Continued).

TABLE 1
Response Surface Variables

q'' (kW/m ²)	$X1$	$X2$	$X3$	$X4$
350	-1	1	1	-1
325	-1	0.257	1	-1
360	-1	1	1	-0.5
362	-1	0.257	1	-0.5
470	0.034	-0.583	-1	0
424	0.034	-1	-1	0
600	0.034	-0.583	-1	0.5
472	0.034	-1	-1	0.5
630	0.034	-0.583	-1	1
580	0.034	-1	-1	1
266	-0.546	1	1	-1
254	-0.546	0.257	1	-1
525	1	-0.583	-1	0.5
408	1	-1	-1	0.5
382	1	-0.583	-1	0
351	1	-1	-1	0

TABLE 2
Response Surface Parameter Coefficients

<i>Parameter</i>	<i>Parameter estimate from coded data</i>
$X1$	-107.427 822
$X2$	97.499 757
$X3$	-181.213 835
$X4$	105.616 097
$X1 * X1$	29.478 552
$X2 * X1$	8.068 647
$X2 * X2$	-42.412 950
$X3 * X1$	0
$X3 * X2$	0
$X3 * X3$	0
$X4 * X1$	22.774 327
$X4 * X2$	25.964 075
$X4 * X3$	-112.160 379
$X4 * X4$	-40.000 000
Intercept	375.207 149

TABLE 3
Response Surface Distribution (response surface
for variable Y: heat flux)

Response mean	422.437 500
Root MSE	32.044 465
R-square	0.979 1
Coefficient of variation	7.585 6

TABLE 4
Significance Estimates by Term

Regression	Degrees of freedom	Type I sum of squares	R-square	F-ratio	Probability >F
Linear	4	181.256	0.921 2	44.129	0.001 5
Quadratic	3	9.919	0.050 4	3.220	0.144 1
Cross-product	4	1.476.729 963	0.007 5	0.360	0.827 2
Total regression	11	192.653	0.979 1	17.056	0.007 3

TABLE 5
Significance Estimates by Parameter

Factor	Degrees of freedom	Sum of squares	Mean square	F-ratio	Probability >F
X1	4	17.324	4.331.065 991	4.218	0.096 1
X2	4	14.104	3.526.027 282	3.434	0.129 7
X3	2	11.173	5.586.611 681	5.441	0.072 3
X4	5	35.711	7.142.208 889	6.955	0.041 8
Total error	4	107.390 871	1.026.847 718		

TABLE 6
Significance Estimates for Model

Parameter	Degrees of freedom	Parameter estimate	Standard error	T for H0: parameter = 0	Probability > T
Intercept	1	375.207 149	82.087 540	4.571	0.010 3
X1	1	-107.427 822	44.635 011	-2.407	0.073 8
X2	1	97.499 757	56.074 033	1.739	0.157 1
X3	1	-181.213 835	73.819 905	-2.455	0.070 1
X4	1	105.616 097	72.173 759	1.463	0.217 2
X1 * X1	1	29.478 552	74.783 935	0.394	0.713 6
X2 * X1	1	8.068 647	94.323 346	0.0855	0.935 9
X2 * X2	1	-42.412 950	76.395 537	-5.555	0.608 4
X3 * X1	0	0	—	—	—
X3 * X3	0	0	—	—	—
X3 * X2	0	0	—	—	—
X3 * X2	1	22.774 327	93.825 500	0.243	0.820 2
X4 * X2	1	25.964 375	106.128 174	0.245	0.818 8
X4 * X3	1	-112.160 379	193.289 372	-0.580	0.592 9
X4 * X4	1	-40.000 000	111.005 282	-0.360	0.736 8

an uncertainty analysis, finding the uncertainty in the maximum heat release rate due to uncertainty in the input parameter range. For a normal range of parameters the response surface gives reasonable results, especially in terms of the relatively low accuracy requirements of a PRA.

The response surface can be used to predict a distribution of the maximum heat release rate given a scenario and distributions of the parameters. This distribution can then be used with predictive methods for heat release rate curves to determine a heat release curve for a scenario for which no experimental data are available. Future work would include the calculation of the heat release curves and their probability distributions from an uncertainty analysis of the response surface. Since a response surface cannot be better than the underlying code, response surfaces should also be developed from existing, more detailed, computer codes, such as FAST/FFM.^{7,9} The use of such codes would also allow the modeling of more complex surfaces. The curves would then be integrated into a compartment fire model for the purpose of determining the growth time and the hazard time, and, eventually, the risk due to fire for a given scenario.

ACKNOWLEDGMENT

This work was supported by the Center for Fire Research of the NIST under grant No. 6ONANB9D0947.

REFERENCES

1. Kazarians, M., Siu, N. O. & Apostolakis, G., Fire risk analysis for nuclear power plants: Methodological developments and applications. *Risk Analysis*, **5** (1985) 33-51.
2. Clarke, F. B., Bukowski, R. W., Stiefel, S. W., Hall, Jr, J. R. & Steele, S. A., A method to predict fire risk: The report of the National Fire Protection Research Foundation Risk Project. In *Report to the National Fire Protection Research Foundation (NFPRF)*. NFPRF, Quincy, MA, 1990. (Developed at Benjamin/Clarke Associates, National Institute of Standards and Technology, and the National Fire Protection Association.)
3. Brandyberry, M. D. & Apostolakis, G. E., Fire risk analysis methodology: Initiating events. Report NIST-GCR-89-562, National Institute of Standards and Technology Centre for Fire Research, Gaithersburg, MD 1989.
4. Brandyberry, M. D. & Apostolakis, G. E., Fire risk in buildings: Frequency of Exposure and physical models. *Fire Safety J.*, **17** (1991) 339-61.

5. Brandyberry, M. D. & Apostolakis, G. E., Fire risk in buildings: Scenario definition and ignition frequency calculations, *Fire Safety J.*, **17** (1991) 363–86.
6. Bukowski, R. W., *An Introduction to Fire Hazard Modeling*. NBSIR 86-3349, National Institute of Science and Technology, Gaithersburg, MD, 1986.
7. Dietenberger, M. A., Furniture fire model, Report NBS-GCR-84-480. National Bureau of Standards Center for Fire Research, Gaithersburg, MD, 1984.
8. Dietenberger, M. A., A validated furniture fire model with FAST (HEMFAST). Report NIST-GCR-89-564, National Institute of Standard and Technology Center for Fire Research, Gaithersburg, MD, 1989.
9. Dietenberger, M. A. Technical reference and user's guide for FAST/FFM Version 3. Report NIST-GCR-91-589, National Institute of Standards and Technology, Building and Fire Research Laboratory, Gaithersburg, MD, 1991.
10. Brandyberry, M. & Apostolakis, G., Response surface approximation of a fire risk analysis computer code. *Reliability Engineering & System Safety*, **29** (1990) 153–84.
11. Olivi, L. (ed.), *Response Surface Methodology: Handbook for Nuclear Reactor Safety*. UER 9600 EN, Commission of the European Communities, Ispan, Italy, 1984.
12. Babrauskas, V & Krasny, J., *Fire Behavior of Upholstered Furniture*. NBS Monograph 173, National Bureau of Standards, Gaithersburg, MD, 1985.
13. Quintiere, J., Burning rates. In *SPFE Handbook of Fire Protection Engineering* (1st edn). National Fire Protection Association, Quincy, MA, 1988.
14. Drysdale, D., *An Introduction to Fire Dynamics*. John Wiley, New York, 1985.
15. Delichatsios, M. A., Burning and upward flame spread on vertical material surfaces: An outline of a comprehensive simulation model and simplified correlations. FMRC Technical Report, FMRC J.I. 0Q0J1.BU FMRC, Norwood, MA, 1988.
16. Fernandez-Pello, A. C. & Santoro, R. J., On the dominant mode of heat transfer in downward flame spread. In *17th Symposium (International) on Combustion*. The Combustion Institute, Pittsburgh, PA, 1980, pp. 1201–9.
17. Fernandez-Pello, A. C., Ray, S. R. & Glassman, I., An analysis of the heat transfer mechanisms in horizontal flame propagation. In *18th Symposium (International) on Combustion*. The Combustion Institute, Pittsburg, PA, 1981.
18. Quintiere, J., Surface flame spread. In *SPFE Handbook of Fire Protection Engineering* (1st edn). National Fire Protection Association, Quincy, MA, 1988.
19. de Ris, J. N., Spread of a laminar diffusion flame. In *12th Symposium (International) on Combustion*. The Combustion Institute, Pittsburgh, PA, 1969, pp. 241–52.
20. Quintiere, J. G. & Harkleroad, M., *New Concepts for Measuring Flame Spread Properties* US Department of Commerce, NBSIR 84-2943, 1984.

21. Markenstein, G. H. & de Ris, J. N., Upward fire spread over textiles. In *14th Symposium (International) on Combustion*. The Combustion Institute, Pittsburgh, PA, 1973.
22. Fernandez-Pello, A. C., Upward laminar flame spread under the influence of externally applied thermal radiation. *Combustion Sci & Technol.*, **17** (1977) 87-98.
23. Orloff L., de Ris, J. N. & Markenstein, G. H., Upward turbulent fire spread and burning of fuel surfaces. In *15th Symposium (International) on Combustion*. The Combustion Institute, Pittsburgh, PA, 1974.
24. Orloff, L., Modak, A. T. & Alpert, R. L., Burning of large scale vertical surfaces. In *16th Symposium (International) on Combustion*. The Combustion Institute, Pittsburgh, PA, 1976.
25. Annamalai, A.K. & Sibulkin, M., Flame spread over combustible surfaces for laminar flow systems, Part I: Excess fuel and heat flux. *Combustion Sci. & Technol.*, **19** (1979) 167-83.
26. Annamalai, A.K. & Sibulkin, M., Flame spread over combustible surfaces for laminar flow systems, Part II: Flame heights and fire spread rates. *Combustion Sci. & Technol.*, **19** (1979) 185-93.